[9] G. Satoh, "Stabilized microstrip oscillator using dielectric resonator," in *Proc. 1974 IEEE Int. Solid-State Circuits Conf.*, Feb. 1974, pp. 184–185.
[10] T. Makino and A. Hashima, "A highly stabilized MIC Gunn oscillator using a dielectric resonator," *IEEE Trans. Microwave Theory Tech.*, vol. MTT-27, pp. 633–638, July 1979.
[11] S. Shinozaki, T. Hayasaka, and K. Sakamoto, "6–12 GHz transmission type dielectric resonator transistor oscillators," in *1978 IEEE MTT-S Int. Microwave Symp. Dig.*, June 1978, pp. 294–299.
[12] H. Komizo and Y. Tokumitsu, "Millimeter wave integrated circuits," in *1981 IEEE MTT-S Int. Microwave Symp. Dig.*, June 1981, pp. 179–181.
[13] K. Kohiyama and K. Momma, "Band reflection type cavity stabilized Gunn oscillator," *Trans. Inst. Electron. Commun. Eng. Japan*, vol. 57–B, no. 2, pp. 98–105, Feb. 1974.
[14] N. Imai and K. Yamamoto, "A design of high-Q dielectric resonators for MIC applications," *Trans. Inst. Electron. Commun. Eng. Japan*, vol. J67-B, no. 5, pp. 497–504, May 1984.
[15] R. R. Bonetti and A. Atia, "Design of cylindrical dielectric resonators in inhomogeneous media," *IEEE Trans. Microwave Theory Tech.*, vol. MTT-29, pp. 323—326, Apr. 1981.
[16] W. E. Courtney, "Analysis and evaluation of a method of measuring the complex permittivity and permeability of microwave insulators," *IEEE Trans. Microwave Theory Tech.*, vol. MTT-18, pp. 476–485, Aug. 1970.
[17] J. E. Aitken, P. H. Ladbrooke, and M. H. N. Potok, "Microwave measurement of the temperature coefficient of permittivity for sapphire and alumina," *IEEE Trans. Microwave Theory Tech.*, vol. MTT-23, pp. 526–529, June 1975.
[18] T. Makino, "Temperature dependence and stabilization conditions of an MIC Gunn oscillator using a dielectric resonator," *Trans. Inst. Electron. Commun. Eng. Japan*, vol. 62-B, no. 4, pp. 352–358, Apr. 1979.

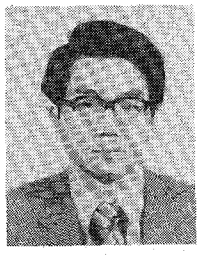

Nobuaki Imai was born in Kochi, Japan, in 1953. He received the B.S. degree in electrical engineering from Nagoya Institute of Technology, Nagoya, Japan, in 1975, and the M.S. degree from Kyoto University, Kyoto, Japan, in 1977.

He joined Yokosuka Electrical Communication Laboratories, Japan, in 1977, and has been engaged in the research of millimeter-wave integrated circuits.

Mr. Imai is a member of the Institute of Electronics and Communication Engineers of Japan.

Kazuyuki Yamamoto was born in Kyoto, Japan, on July 13, 1946. He received the B.S., M.S., and Ph.D. degrees in electrical engineering, from the University of Kyoto, Japan, in 1969, 1971, and 1982, respectively.

Since joining the Electrical Communication Laboratory, Nippon Telegraph and Telephone Public Corporation (NTT), Tokyo, Japan, in 1971, he has been engaged in the research and development of filters, solid-state circuits, and transmission lines for millimeter and submillimeter wavelength regions. He is currently engaged in the research and development of millimeter-wave integrated circuits for radio communication systems.

Dr. Yamamoto is a member of the Institute of Electronics and Communication Engineers of Japan.

Boundary Element Method Approach to Magnetostatic Wave Problems

KEN'ICHIRO YASHIRO, MEMBER, IEEE, MORIYASU MIYAZAKI, AND SUMIO OHKAWA, SENIOR MEMBER, IEEE

Abstract — **In this paper, the technique for application of the boundary element method (BEM) to analysis of magnetostatic waves (MSW's) is established. To show the availability of the technique, two types of waveguides for the MSW are studied; one is a waveguide constituting a YIG slab shielded with metal plates and the other is a waveguide consisting of an unshielded YIG slab. With the former structure the results obtained by the present technique are compared with the analytical solutions, and with the latter the BEM is compared with Marcatili's approximate method since there is no analytical solution in this case. Those comparisons are performed successfully for both cases.**

The paper concludes that the BEM is useful and effective for analysis of a wide range of MSW problems.

Manuscript received April 9, 1984; revised October 23, 1984.

K. Yashiro and S. Ohkawa are with the Department of Electronic Engineering, Chiba University, 1-33, Yayoi-cho, Chiba, 260 Japan.

M. Miyazaki is with Mitsubishi Electric Corp., Kamakura, Japan.

I. Introduction

SEVERAL TYPES OF waveguides for magnetostatic waves (MSW's) have so far been proposed and solved analytically [1]–[3]. Most of them, however, have a simple geometry; as a matter of fact, we may say that an analytical solution can be given only for structures of simple geometry. But from the practical point of view, a numerical solution which can be applied to arbitrary structures is required for an analysis of the MSW problems.

The integral equation formulation has proved to be a powerful tool for obtaining rigorous solutions of electromagnetic and acoustic wave problems. The boundary element method (BEM) [4]–[6] is often used for the calculation of scattering and propagation problems. The BEM is one representative of integral methods and is equivalent to

0018-9480/85/0300-0248$01.00 ©1985 IEEE

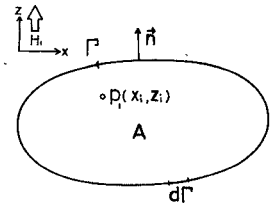

Fig. 1. Two-dimensional model. H_i is a biasing magnetic field.

the moment method with subsectional bases and Dirac delta functions as testing functions [7]. In this paper, a general computer program is developed for solving a wide range of MSW problems.

For the purpose of analysis of waveguides for MSW's, the authors have established an approach using the BEM. First, the boundary integral equation for the MSW problem is derived and the fundamental solution which is defined as a solution in infinite space corresponding to a point source is obtained.

Subsequently, we have dispersion curves and magnetic potential distributions of magnetostatic surface waves (MSSW's) for two different types of waveguides, i.e., a shielded YIG slab and an unshielded YIG slab. For the former structure, a good agreement with the analytical solution [1], [8], [9] is shown, and for the latter a comparison with the solution by Marcatili's approximate method [10] is also shown to give reasonable agreement.

II. Formulation

When a biasing magnetic field, which is assumed to be uniform for mathematical simplicity, is applied to yttrium iron garnet (YIG) along the z-axis, MSW can propagate along the y-axis, as shown in Fig. 1. Assuming a quasistatic approximation and that the MSW varies as $\phi(x, z)e^{j(\omega t-\beta y)}$, the magnetic potential of the MSW ϕ satisfies the following equation:

$$\mu\frac{\partial^2\phi}{\partial x^2}+\frac{\partial^2\phi}{\partial z^2}-\mu\beta^2\phi=0 \tag{1}$$

where μ is the diagonal component of tensor permeability of YIG.

By using Green's formula, the potential at the arbitrary point P_i inside region A is given as

$$\phi(P_i)=\int_\Gamma\phi_i^*\left(\mu\frac{\partial\phi}{\partial x}n_x+\frac{\partial\phi}{\partial z}n_z\right)d\Gamma - \int_\Gamma\phi\left(\mu\frac{\partial\phi_i^*}{\partial x}n_x+\frac{\partial\phi_i^*}{\partial z}n_z\right)d\Gamma \tag{2}$$

where Γ is a boundary contour around the region A, $n_x(n_z)$ is the x (z) component of the unit normal vector $\vec{n}$ to Γ, and ϕ_i^* is a fundamental solution, which is

$$\phi_i^*=\frac{1}{2\pi\sqrt{\mu}}K_0(\beta r) \tag{3}$$

following the usual manner [11] for the case of MSSW, where

$$r=\sqrt{(x-x_i)^2+\mu(z-z_i)^2} \tag{4}$$

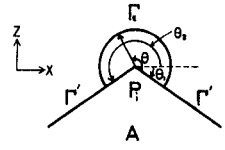

Fig. 2. Expanded view in the vicinity of P_i when P_i is on the boundary. Γ_ϵ is a indented integral contour, where the distance from P_i to Γ_ϵ is ϵ.

and K_0 is the zeroth-order modified Bessel function of the second kind. If P_i is on the boundary, (2) leads to the following boundary integral equation:

$$C^i\phi(P_i)=\int_\Gamma\phi_i^*\left(\mu\frac{\partial\phi}{\partial x}n_x+\frac{\partial\phi}{\partial z}n_z\right)d\Gamma - \int_\Gamma\phi\left(\mu\frac{\partial\phi_i^*}{\partial x}n_x+\frac{\partial\phi_i^*}{\partial z}n_z\right)d\Gamma \tag{5}$$

where C^i is given by

$$C^i=1-\frac{1}{2\pi}\left\{\tan^{-1}\left(\sqrt{\mu}\tan\theta_2\right)-\tan^{-1}\left(\sqrt{\mu}\tan\theta_1\right)\right\}. \tag{6}$$

Here θ_1 and θ_2 are angles between the x-axis and the tangent to the boundary at P_i, as illustrated in Fig. 2, and $\tan^{-1}x$ means a normal value, i.e., $\tan^{-1}x=n\pi+\mathrm{Tan}^{-1}x$ ($\mathrm{Tan}^{-1}x$; principal value).

Though (5) is a usual expression for the boundary integral equation, it is inconvenient for putting in the boundary conditions for the present case. Thus, we use a technique of adding/subtracting $\phi\phi_i^*\kappa\beta n_x$ to/from the integrand in the right-hand side of (5), where κ is an off-diagonal component of tensor permeability. As a result, we obtain the desirable boundary integral equation as follows:

$$C^i\phi(P_i)=\int_\Gamma\phi_i^*q\,d\Gamma-\int_\Gamma\phi q_i^*\,d\Gamma \tag{7}$$

where

$$q=\left(\mu\frac{\partial\phi}{\partial x}-\kappa\beta\phi\right)n_x+\frac{\partial\phi}{\partial z}n_z$$

$$q_i^*=\left(\mu\frac{\partial\phi_i^*}{\partial x}-\kappa\beta\phi_i^*\right)n_x+\frac{\partial\phi_i^*}{\partial z}n_z.$$

q and q_i^* mean the normal components of the magnetic flux density. The boundary conditions are introduced through the values of ϕ and q along the boundary contour.

The next step is to discretize (7). For this purpose, divide the boundary Γ into N elements so that (7) becomes

$$C^i\phi(P_i)=\sum_{j=1}^{N}\int_{\Gamma_j}\phi_i^*q\,d\Gamma-\sum_{j=1}^{N}\int_{\Gamma_j}\phi q_i^*\,d\Gamma \tag{8}$$

where the observation point P_i coincides with the ith boundary node. If we apply linear elements to (8), ϕ, q, x, and z on jth element are expressed as follows:

$$\left.\begin{aligned}\phi(\xi)&=\psi_1\phi_j+\psi_2\phi_{j+1}\\ q(\xi)&=\psi_1q_j+\psi_2q_{j+1}\\ x(\xi)&=\psi_1x_j+\psi_2x_{j+1}\\ z(\xi)&=\psi_1z_j+\psi_2z_{j+1}\end{aligned}\right\} \tag{9}$$

where ϕ_j and q_j are ϕ and q at the jth boundary node, respectively. ψ_1 and ψ_2 are called interpolation functions which are defined for convenience of numerical integration as follows:

$$\left.\begin{aligned}\psi_1(\xi) &= 1-\xi \\ \psi_2(\xi) &= \xi\end{aligned}\right\} \qquad (0 \leqslant \xi \leqslant 1) \tag{10}$$

in the case where the boundary element $\Gamma_j (j = i)$ includes the observation point P_i, and

$$\left.\begin{aligned}\psi_1(\xi) &= (1-\xi)/2 \\ \psi_2(\xi) &= (1+\xi)/2\end{aligned}\right\} \qquad (-1 \leqslant \xi \leqslant 1) \tag{11}$$

for an integral along the element Γ_j which does not include the point P_i. Substituting (9) into (8) leads to

$$\sum_{j=1}^{N} H_{ij}\phi_j = \sum_{j=1}^{N} G_{ij} q_j \tag{12}$$

where

$$\left.\begin{aligned}H_{ij} &= \int_{\Gamma_{j-1}} \psi_2 q_i^*\, d\Gamma + \int_{\Gamma_j} \psi_1 q_i^*\, d\Gamma + C^i \delta_{ij} \\ G_{ij} &= \int_{\Gamma_{j-1}} \psi_2 \phi_i^*\, d\Gamma + \int_{\Gamma_j} \psi_1 \phi_i^*\, d\Gamma\end{aligned}\right\}. \tag{13}$$

Most of the integrations in (13) can be calculated using the Gaussian integration formula. But an integration where its path includes an observation point should be calculated analytically as far as possible. For instance, $\int_{\Gamma_i} \psi_1 \phi_i^*\, d\Gamma$ is calculated as follows:

$$\begin{aligned}\int_{\Gamma_i} \psi_1 \phi_i^*\, d\Gamma &= -\frac{|\Gamma_i|}{2\pi\sqrt{\mu}} \int_0^1 (\xi - 1) K_0(\beta r_i \xi)\, d\xi \\ &= -\frac{|\Gamma_i|}{2\pi\sqrt{\mu}} \left\{ \frac{1}{(\beta r_i)^2} - \frac{1}{\beta r_i} K_1(\beta r_i) \right. \\ &\quad \left. - \int_0^1 K_0(\beta r_i \xi)\, d\xi \right\}\end{aligned}$$

and so forth, where r_i is the value of r when x and z in (4) coincide with the coordinates of both terminals of the ith boundary element and K_1 is the first-order modified Bessel function of the second kind. The integral in the right-hand side is divided into two parts: one is the term with logarithmic singularity and the other is the rest.

Since (12) is satisfied with $i = 1, 2, \cdots, N$, we may express it simply by the following matrix form:

$$H\phi = Gq. \tag{14}$$

If the boundary conditions are applied to the components of ϕ or q vectors, (14) can be solved for the unknowns as simultaneous equations.

If there exist two regions as shown in Fig. 3, we have to derive the system of equations as in (14) for each region. These systems are interconnected by the boundary conditions between regions I and II, i.e., ${}_{\mathrm{I}}\phi_{\mathrm{II}} = {}_{\mathrm{II}}\phi_{\mathrm{I}}$, ${}_{\mathrm{I}}q_{\mathrm{II}} = -{}_{\mathrm{II}}q_{\mathrm{I}}$, where ${}_{\mathrm{I}}\phi_{\mathrm{II}}$, for instance, stands for the value of ϕ at the point P corresponding to P_j in region I interfaced with region II. The minus sign before ${}_{\mathrm{II}}q_{\mathrm{I}}$ means that the normal vector on the boundary of region I is opposite in direction to that of region II.

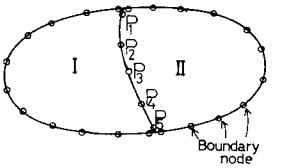

Fig 3. Two-dimensional model consisting of two regions.

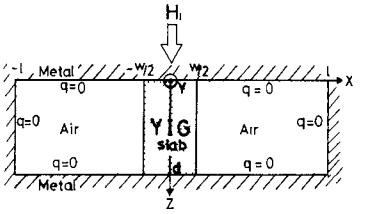

Fig. 4. YIG slab shielded with metal plates.

At the corner, where the normal vector cannot be defined uniquely, two boundary nodes are located in the vicinity close to it. In practice, these two nodes should be taken at the vertex, although the unit normal at each node is the same as that at any other point on each element.

III. Numerical Results and Discussion

A. A Shielded YIG Slab

Let us consider a closed structure for MSSW propagation: in other words, a YIG slab shielded with metal plates as shown in Fig. 4. As mentioned in the previous section, the biasing magnetic field is applied along the z-axis and the MSSW propagates along the y-axis. In this case, the region is divided into three homogeneous subregions, namely, a YIG region and two air ones. The following boundary conditions are imposed: The normal component of the magnetic flux density q vanishes at the metal surface, and the magnetic potential ϕ and the normal component of the magnetic flux density q are continuous at the interface between a YIG slab and an air region. The width and the thickness of the slab are w and d, respectively. The distance between the surface of the YIG slab and the metal plate is l. The following numerical values are used for the computation: gyromagnetic ratio $\gamma = 2.8$ MHz/Oe, the biasing magnetic field $H_i = 251$ Oe, and the saturation magnetization of YIG $4\pi M_s = 1760$ G.

The dispersion relation of a uniform MSSW mode, whose amplitude is independent of z, is shown in Fig. 5, with $w = 5.0$ μm, $l/\lambda_0 = 3.0$, and the number of boundary nodes $N = 90$, where λ_0 is the wavelength obtained analytically. The solid line means the analytical solution, and the symbols $\circ$ and $\times$ indicate the solutions obtained by the BEM, with $d/\lambda_0 = 1.0$ and 2.8, respectively. The solutions by the BEM agree very well with the analytical ones. However, the $\circ$ symbols do not fit on the solid line as well as the $\times$ symbols do. For example, for frequency $f = 3.0$ GHz, the $\circ$ mark deviates from the solid line by about 1.0

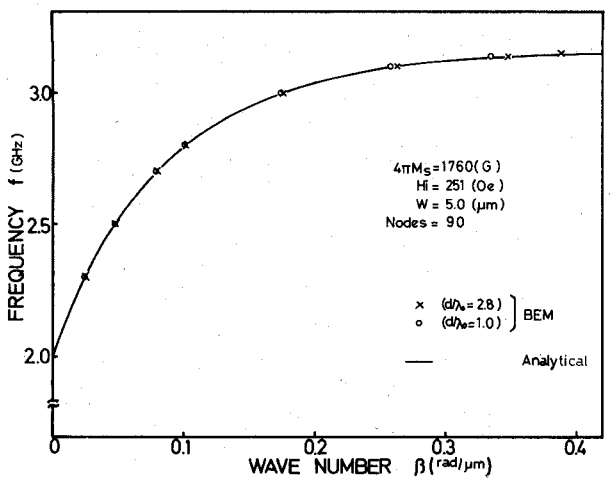

Fig. 5. Dispersion curve for MSSW on shielded YIG slab.

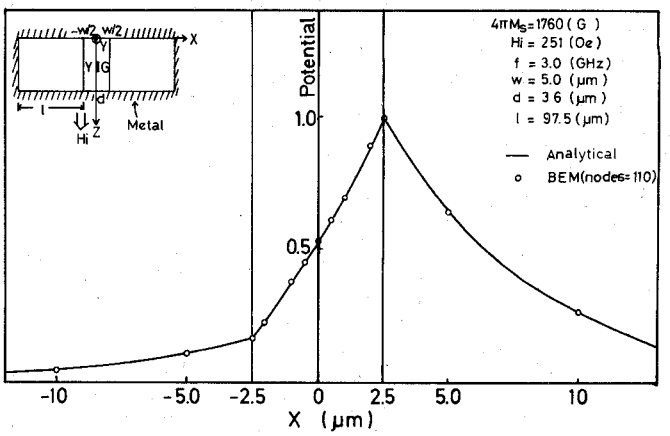

Fig. 7. Potential distribution along the x-axis for MSSW on the shielded YIG slab. The potential is normalized such that the maximum value equals unity.

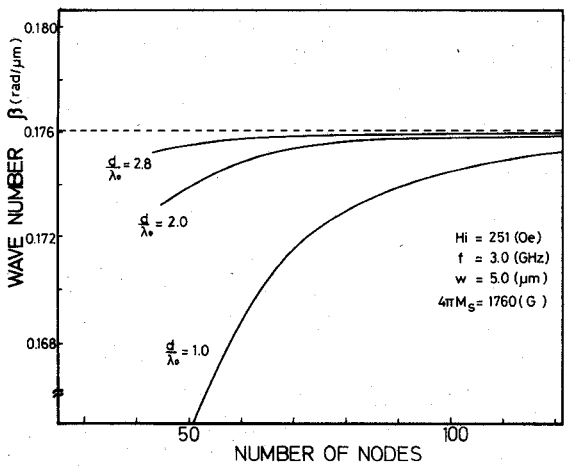

Fig. 6. Relationship between the number of boundary nodes N and the wavenumber β. The broken line indicates the analytical solution.

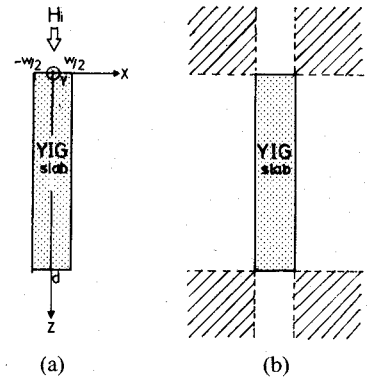

Fig. 8. (a) Unshielded YIG slab. (b) Illustration for Marcatili's approximate method. Potential in the shaded areas is not taken into account.

percent, while the × mark does by about 0.06 percent. Moreover, note that the bigger the wavenumber β, the larger the discrepancy between the solutions.

Fig. 6 shows the relationship between the number of boundary nodes N and the wavenumber β, where the frequency is kept constant (3.0 GHz) with the parameters of $d/\lambda_0 = 1.0$, 2.0, and 2.8. It is clear that the numerical solutions for β by the BEM approach asymptotically to the analytical solution $\beta = 0.17605$ rad/μm as N increases. These results show that the numerical accuracy of the BEM improves as the thickness of YIG slab d increases. This seems to be due to the fact that better uniformity of the wave amplitude along the z-axis is provided by increasing d from the point of numerical computations in the BEM.

The magnetic potential distribution of the MSSW for $f = 3.0$ GHz, $d = 36$ μm ($d/\lambda_0 \doteqdot 1.0$) is shown in Fig. 7. Here we increased the number of boundary nodes to 110, since computation of a potential converges less slowly than computation of a wavenumber. The solid line and the ○ symbols are obtained by the analytical solution and the BEM, respectively. The results show that both solutions are in good agreement.

B. An Unshielded YIG Slab

We will investigate the MSSW which propagates along the y-axis on an unshielded YIG slab magnetized in the z-direction, as shown in Fig. 8(a). In this case, the area is divided into a YIG region and an air one. The continuity of the magnetic potential ϕ and the normal component of the magnetic flux density q is imposed at the boundary between them. It is almost impossible to solve this problem analytically, so the results by the BEM will be compared with the solutions by Marcatili's approximate method [10], in which the shaded areas illustrated in Fig. 8(b) are ignored, since the potential is expected to decay very fast in these areas. The following numerical values are used for the computation: $H_i = 500$ Oe, $w = 100$ μm, and $d = 5000$ μm.

The dispersion relation is shown in Fig. 9. The solid line indicates the solution by Marcatili's approximate method, and the symbols ○ ($N = 28$) and × ($N = 44$) indicate the solutions by the BEM. It is adequate to choose $N = 44$, as is seen from the figure. The × symbols nearly fit on the solid line. In the range of small wavenumbers, however, a slight gap occurs between them. When a wavenumber is small, the potential decays slowly, and hence the shaded areas in Fig. 8(b) must be taken into account. The effect of

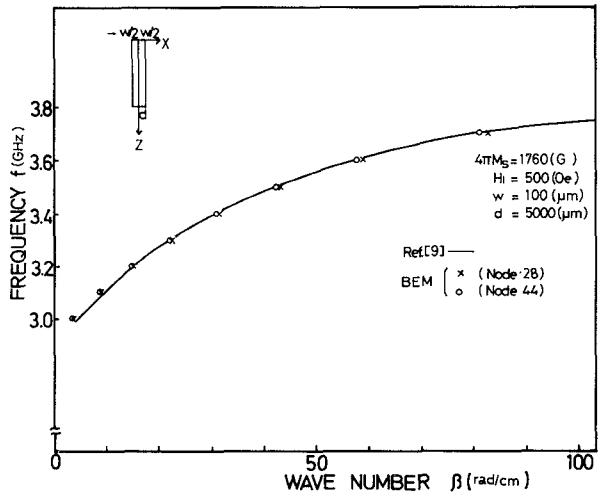

Fig. 9. Dispersion curve for MSSW on the unshielded YIG slab.

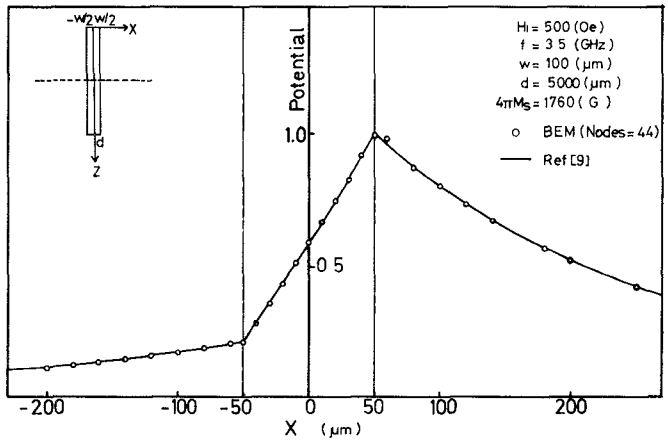

Fig. 10. Potential distribution at $z = d/2$ along the x-axis for MSSW on the unshielded YIG slab. The potential is normalized such that the maximum value all through the area equals unity.

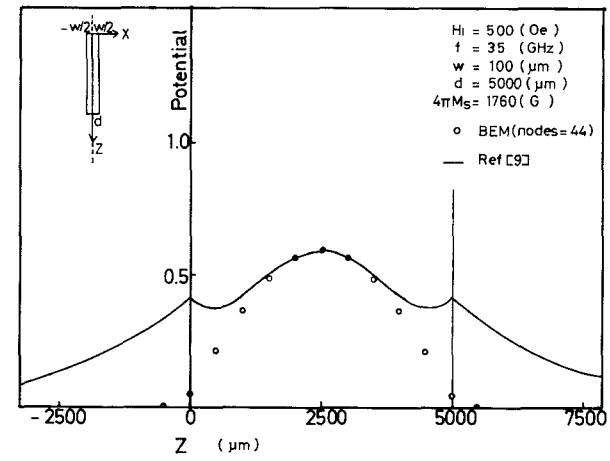

Fig. 11. Potential distribution at $x = 0$ along the z-axis for MSSW on the unshielded YIG slab. The potential is normalized such that the maximum value all through the area equals unity.

the shaded areas is revealed more obviously on the magnetic potential distribution than it appears on the dispersion curve.

Figs. 10 and 11 show the magnetic potential distributions at $z = d/2$ along the x-axis and at $x = 0$ along the z-axis, respectively. The solid lines indicate the solutions by Marcatili's approximate method, and the ∘ symbols mean the solutions by the BEM with $N = 44$. While both the results to represent the potential distributions along the x-axis agree fairly well, those along the z-axis do not show a good agreement except in the vicinity of the center of the slab. It seems that the results by the BEM are more reasonable than those by Marcatili's approximate method, because the potential at the edge of the slab ($z = 0, d$) should not be computed by ignoring the shaded areas; at the same time, this brings the fact that the solid line (the potential curve) does not likely vary continuously passing by around the corner, collating Fig. 10 with Fig. 11.

IV. Conclusions

The technique for applying the BEM to the MSW problem has been studied. The boundary integral equation of the MSW and the fundamental solution of the MSW were obtained, and the discrete formulation of this boundary integral equation was worked out.

In order to show that this technique is available for a wide range of MSW problems, the dispersion curves and the potential distributions for the MSSW's were calculated for two typical examples: one was a shielded YIG slab as an example of a closed structure, and the other was an unshielded YIG slab as an example of an open structure. Both the cases compared well with the analytical solution and with Marcatili's approximate solution, respectively. The authors conclude that the present technique using the BEM is very effective and useful for the analysis of the MSW problems.

References

[1] W. L Bongianni, "Magnetostatic propagation in a dielectric layered structure," *J. Appl. Phys.*, vol. 43, pp. 2541–2548, June 1972.

[2] K. Yashiro and S. Ohkawa, "Guided magnetostatic waves of the YIG plate magnetized nonuniformly," *IEEE Trans. Microwave Theory Tech.*, vol. MTT-29, pp. 745–747, July 1981.

[3] M Uehara, K. Yashiro, and S. Ohkawa, "Guided magnetostatic surface waves on a metallic strip line," *J. Appl. Phys.*, vol. 54, pp. 2582–2587, May 1983.

[4] C. A. Brebbia, *The Boundary Element Method for Engineers.* London: Pentech Press, 1978.

[5] S. Washisu and I. Fukai, "An analysis of electromagnetic unbounded field problems by boundary element method," *IECE Japan*, vol. J64-B, pp. 1359–1365, Dec. 1981.

[6] K. Yashiro and S. Ohkawa, "Application of the boundary element method to plane wave scattering problems from several dielectric cylinders," *IECE Japan*, vol. E67, pp. 170–171, Mar. 1984.

[7] R. F. Harrington, *Field Computation by Moment Methods.* New York, NY: Macmillan, 1968.

[8] R. W. Damon and J. R. Eshbach, "Magnetostatic modes of a ferromagnet slab," *J Phys. Chem. Solids*, vol. 19, nos. 3/4, pp. 308–320, 1961.

[9] K. Kawasaki and M. Umeno, "Influence of surface metallization on the propagation characteristics of surface magnetostatic waves in an axially magnetized rectangular YIG rod," *IEEE Trans. Microwave Theory Tech.*, vol. MTT-22, pp. 391–394, Apr. 1974.

[10] E. A. J. Marcatili, "Dielectric rectangular waveguide and directional coupler for integrated optics," *Bell Syst. Tech. J.*, 2071–2102, Sept. 1969.

[11] C. A. Brebbia, *Progress in Boundary Element Methods*, vol. 1. London: Pentech Press, 1981, pp 13–44.

Ken'ichiro Yashiro (M'83) was born in Osaka, Japan, on May 5, 1950. He received the B.S. and M.S. degrees in electronic engineering from Chiba University, Chiba, Japan, in 1974 and 1976, respectively, and the Ph.D. degree from Tokyo Institute of Technology, Tokyo, Japan, in 1979.

He joined the Department of Electronic Engineering, Chiba University, as a Research Associate in 1979, and has been engaged in research of acoustic and magnetostatic wave devices.

Dr. Yashiro is a member of the Institute of Electronics and Communication Engineers of Japan.

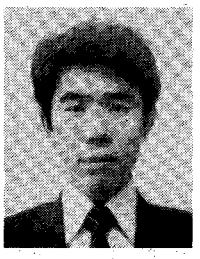

Moriyasu Miyazaki was born in Tokyo, Japan, on July 3, 1959. He received the B.E. degree in electrical engineering and the M.E. degree in electronic engineering from Chiba University, Chiba, Japan, in 1982 and 1984, respectively.

He joined Mitsubishi Electric Corp., Kamakura, Japan, in 1984. He was engaged in the application of MSW to MIC at Chiba University. His current interests are in space communication engineering and electromagnetic wave-scattering problems.

Mr. Miyazaki is a member of the Institute of Electronics and Communication Engineers of Japan.

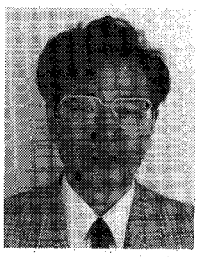

Sumio Ohkawa (M'82–SM'84) was born in Hokkaido, Japan, on July 16, 1935. He received the B.Eng. degree in electrical engineering from Chiba University, Chiba, Japan, in 1961, and the D.Eng. degree from Tokyo Institute of Technology, Tokyo, Japan, in 1974.

He joined the Department of Electrical Engineering of Chiba University as a Research Associate after graduating. In 1970, he transferred to the Department of Electronic Engineering as an Associate Professor, and in 1978 was promoted to full Professor. From October 1979 to June 1980, he studied at the Microwave Research Institute, Polytechnic Institute of New York as a Visiting Professor sent abroad by the Ministry of Education of Japan. His research has chiefly been concerned with measurements of materials in the microwave range. He is now also interested in the applications of magnetostatic waves to microwave integrated circuits.

Dr. Ohkawa is a member of the Institute of Electronics and Communication Engineers of Japan.

Locking Behavior of a Microwave Multiple-Device Ladder Oscillator

SHIGEJI NOGI AND KIYOSHI FUKUI, MEMBER, IEEE

Abstract—**This paper presents a detailed discussion on the injection-locking property of a microwave ladder oscillator which is essentially an array of diode mount-pairs in a rectangular waveguide cavity. It is shown both analytically and experimentally that the use of a ladder structure is advantageous both in obtaining a large locking figure of merit (i.e., $2Q_{ex}^{-1}$) and in rapidity of the transient response to the PSK signal injection.**

I. INTRODUCTION

OWING TO THE increasing demands for high-power microwave generation, various methods have been developed to combine output powers of many active devices. They were well reviewed by K. J. Russel [1] in 1979 and more recently by K. Chang and C. Sun [2] in 1983. In previous papers [3]–[5], the authors proposed a very simple multiple-device structure, i.e., a microwave ladder oscillator, which is essentially an array of diode mount-pairs in a rectangular waveguide, and gave a detailed discussion on the optimum design and successful performance, including a quantitative description of the power-combining mechanism and a mode-analytical discussion of the stable desired-mode operation.

The investigation of the behavior under application of a locking signal must be one of the pertinent problems of such multiple-device oscillators, especially in connection with amplifier application. Kurokawa [6], [7] gave an analytical study using an eigenfunction approach on two multiple-device oscillators of an N-way combining structure (Rucker's [8] and Kurokawa and Magalhaes' [9]). He showed that the locking range and the condition for stable locked operation of such multiple-device oscillators can be given by the expression of the same form as in single-device oscillators, leaving the effect of the number of combined active devices upon the external Q untouched. Experiments on the TM_{ono}-mode cylindrical cavity

Manuscript received February 22, 1984; revised October 30, 1984. This work was supported in part by a Grant in Aid for Fundamental Research from the Ministry of Education, Japan.

The authors are with the Department of Electronics, Okayama University, Okayama 700, Japan.

0018-9480/85/0300-0253$01.00 ©1985 IEEE